A Giant Protease with Potential to Substitute for Some Functions of the Proteasome

Elke Geier,[1] Günter Pfeifer,[2] Matthias Wilm,[3] Maria Lucchiari-Hartz,[1] Wolfgang Baumeister,[2] Klaus Eichmann,[1] Gabriele Niedermann[1]*

An alanyl-alanyl-phenylalanyl-7-amino-4-methylcoumarin–hydrolyzing protease particle copurifying with 26*S* proteasomes was isolated and identified as tripeptidyl peptidase II (TPPII), a cytosolic subtilisin-like peptidase of unknown function. The particle is larger than the 26*S* proteasome and has a rod-shaped, dynamic supramolecular structure. TPPII exhibits enhanced activity in proteasome inhibitor–adapted cells and degrades polypeptides by exo- as well as predominantly trypsin-like endoproteolytic cleavage. TPPII may thus participate in extralysosomal polypeptide degradation and may in part account for nonproteasomal epitope generation as postulated for certain major histocompatibility complex class I alleles. In addition, TPPII may be able to substitute for some metabolic functions of the proteasome.

The proteasome appears to be the major protease of the nuclear and cytoplasmic compartments of the eukaryotic cell. Proteasomal degradation controls the lifetime of most cellular proteins, including many regulatory proteins, and generates peptide antigens for presentation by major histocompatibility complex (MHC) class I molecules to $CD8^+$ cytotoxic T cells (*1*). Proteasome inhibitors are usually lethal for the eukaryotic cell. However, the vital functions of proteasomes may to some extent be redundant: Mouse EL4 lymphoma cells could be adapted to grow in the presence of vinyl sulphone (VS)–proteasome inhibitors at concentrations lethal for most cells (*2*). The adapted cells can degrade ubiquitinated proteins, control the cell cycle, and assemble MHC class I molecules and had enhanced alanyl-alanyl-phenylalanyl-7-amino-4-methylcoumarin (AAF-AMC)–hydrolyzing activity residing in a proteolytic complex larger than proteasomes.

During attempts to purify 26*S* proteasomes from mammalian cell lysates, we detected in high molecular weight (HMW) fractions enormous quantities of AAF-AMC–hydrolyzing activity eluting from Mono Q–anion-exchange columns between 20*S* and 26*S* proteasomes and from Superose 6 size-exclusion columns slightly before the 26*S* proteasomes (Fig. 1A) (*3*, *4*). On silver-stained SDS-polyacrylamide gels, the isolated protease displayed as one predominant band larger in size than any of the proteasome bands (Fig. 1B). This band was excised, cleaved in the gel by trypsin, and analyzed by nano-electrospray tandem mass spectrometry (*5*). The sequences of 11 tryptic fragments unambiguously identified murine tripeptidyl peptidase II (TPPII) (E.C. 3.4.14.10; molecular mass 138 kD) (*6*). TPPII has a membrane-bound (*7*) as well as a HMW cytosolic form and is a serine-peptidase of the subtilisin-type that removes tripeptides from the free NH_2-terminus of oligopeptides (*8*).

Electron microscopic examination of TPPII (*9*) displayed a rod-shaped assembly about 50 nm in length and 17 nm in diameter (Fig. 1C, a). Averages over the whole data set of 1365 individual particles based on a multireference alignment procedure reveal a longitudinal segmentation pattern (inset). All particles are built of eight segments, each ~6.5 nm in width. This indicates that a scaffolding protein participates in the assembly of the particle and determines its length. Because such a protein cannot be detected in the mature particle, it may be degraded during maturation, similar perhaps to the Ump1 protein, which is required for the assembly of yeast 20*S* proteasomes (*10*). An electron-dense stripe running perpendicular to the plane of the eight disks spans the assembly from end-to-end, possibly representing an internal channel. Depending on the size of internal channels or cavities, the total mass of the particle is estimated to be between 5 and 9 MD. Some variations between individual complexes can be discerned; they appear either ovoid (white box in Fig. 1C, a) or dumbbell-shaped (black box in Fig. 1C, a). Eigenvector-eigenvalue image classification (Fig. 1C, b to e) revealed variations in length (47.2 to 51.7 nm) and in the positions of constricted regions. The class averages (Fig. 1C, f to i) show that the constrictions comprise two adjacent segments that may be located centrally (segments 4/5, Fig. 1C, f), terminally (segments 1/2 and 7/8, Fig. 1C, i), or at intermediate positions (for example, segments 2/3, Fig. 1C, g). The coexistence of classes with alternate constrictions suggests that the complex can undergo a peristaltic movement.

Of a panel of fluorogenic proteasome substrates, TPPII rapidly hydrolyzed chymotrypsin- and trypsin-like tripeptidyl substrates with unblocked NH_2-termini (Table 1). The specific activity of TPPII for AAF-AMC is several orders of magnitude higher than that of mouse 20*S* proteasomes or the Tricorn protease (80 pmol μg^{-1} min^{-1}) (*11*). Like Tricorn protease (*11*), TPPII requires a free NH_2-terminus to hydrolyze this substrate efficiently. On the protein level, TPPII is about one-tenth as abundant as proteasomes in unmanipulated EL4 cells, as estimated from the specific activities for fluorogenic substrates. The proteasome inhibitor *N*-acetyl-L-leucinyl-L-leucinal-L-norleucinal (LLnL) does not inhibit TPPII at all, whereas the potent TPPII inhibitor AAF-chloromethylketone (AAF-CMK) shows marginal inhibition of the chymotrypsin-like activity of the proteasome (Fig. 2). Unexpectedly, the AAF-AMC–hydrolyzing activity of TPPII was inhibited by lactacystin, although less efficiently than that of proteasomes.

Next we studied whether TPPII could account for the enhanced HMW AAF-AMC–hydrolyzing activity reported for cells adapted to proteasome inhibitors (*2*). EL4 thymoma cells were cultured in the presence of 6 μM lactacystin, which severely inhibits the chymotrypsin- and trypsin-like activities of

Table 1. Hydrolysis of synthetic substates by murine TPPII and by murine 20*S* proteasomes. Activity was assayed by incubation of 480 ng of purified proteasomes or of 6 ng of purified TPPII with fluorogenic substrates (final concentration, 100 μM, purchased from Bachem or Sigma) for 30 min at 37°C. The fluorescence of AMC or βNA was measured. Suc, succinyl; Z, benzoxycarbonyl; Bz, benzoyl.

Substrate	Specific activity (pmol μg^{-1} min^{-1})	
	TPPII	20*S* proteasomes
H-Ala-Ala-Phe-AMC	14,700	12
Suc-Ala-Ala-Phe-AMC	34	23
H-Phe-AMC	0	0.04
Suc-Leu-Leu-Val-Tyr-AMC	0	51
H-Leu-Val-Tyr-AMC	1100	4.6
Z-Val-Val-Arg-AMC	7	41
Z-Val-Gly-Arg-AMC	0	39
Bz-Ala-Arg-Arg-AMC	0	2.3
H-Ala-Phe-Lys-AMC	2460	1.1
Z-Leu-Leu-Glu-βNA	0	12

[1]Max-Planck Institute of Immunobiology, Stübeweg 51, D-79108 Freiburg, Germany. [2]Max-Planck Institute of Biochemistry, Am Klopferspitz 18a, D-82152 Martinsried, Germany. [3]European Molecular Biology Laboratory, Meyerhofstrasse 1, D-69117 Heidelberg, Germany.

*To whom correspondence should be addressed. E-mail: niedermann@immunbio.mpg.de

the proteasome (*12*), whereas the AAF-AMC–hydrolyzing activity of TPPII is only partially impaired. Although less than 0.1% of the cells survived repeated applications of the proteasome inhibitor, resistant cells grew out after 2 to 3 weeks, with a viability gradually increasing to 70 to 90% after 2 to 3 months. Hydrolysis of proteasome substrates such as Z-GGL-AMC was reduced in adapted cells to about 8 to 30% of that of untreated cells, and AAF-AMC–hydrolyzing activity was enhanced 1.5- to 4.5-fold, as determined at several time points in intact cells or whole-cell lysates of several independent cultures (*13*). The enhanced AAF-AMC–hydrolyzing activity resided in the fraction of HMW cytosolic proteins. On either size-exclusion or anion-exchange columns this enhancement was exclusively at the elution position of TPPII (Fig. 3, A and B). More than 95% of this activity could be depleted with a TPPII-specific antiserum (*13*).

TPPII removes tripeptides stepwise from the free NH_2-terminus of oligopeptides and is classified as a tripeptidyl peptidase (*8*), that is, as an exopeptidase. Although such an enzyme may participate in general protein degradation, it is difficult to envisage the substitution of the multiple functions of proteasomes by an exopeptidase or to rationalize the need for TPPII to have an elaborate supramolecular structure. To determine if TPPII has additional proteolytic activities permitting the degradation of polypeptides into oligopeptides, we studied the digestion of a synthetic 41–amino acid polypeptide corresponding to the ovalbumin amino acid residues 37 to 77 (Fig. 4). Several degradation products of $Ova_{37–77}$ were produced by the tripeptidase activity of TPPII, shortened from the NH_2-terminus by multiples of three residues. A product lacking 24 NH_2-terminal residues was also readily detected, but fragments shortened by 15, 18, or 21 amino acids were not found. The remaining fragments were produced by endoproteolytic cleavage, either as primary products or through intermediates initially produced by the tripeptidyl peptidase activity. Degradation of the COOH-terminal two-thirds of the substrate was almost entirely due to endoproteolytic cleavage, and the velocity of degradation was faster than by proteasomes (80 pmol min^{-1} μg^{-1} versus 5 pmol min^{-1} μg^{-1}). Frequently, but not exclusively, the endoproteolytic cleavage sites were located at the carboxyl side of lysine (K) and arginine (R), suggesting that the endopeptidase activity is predominantly, but

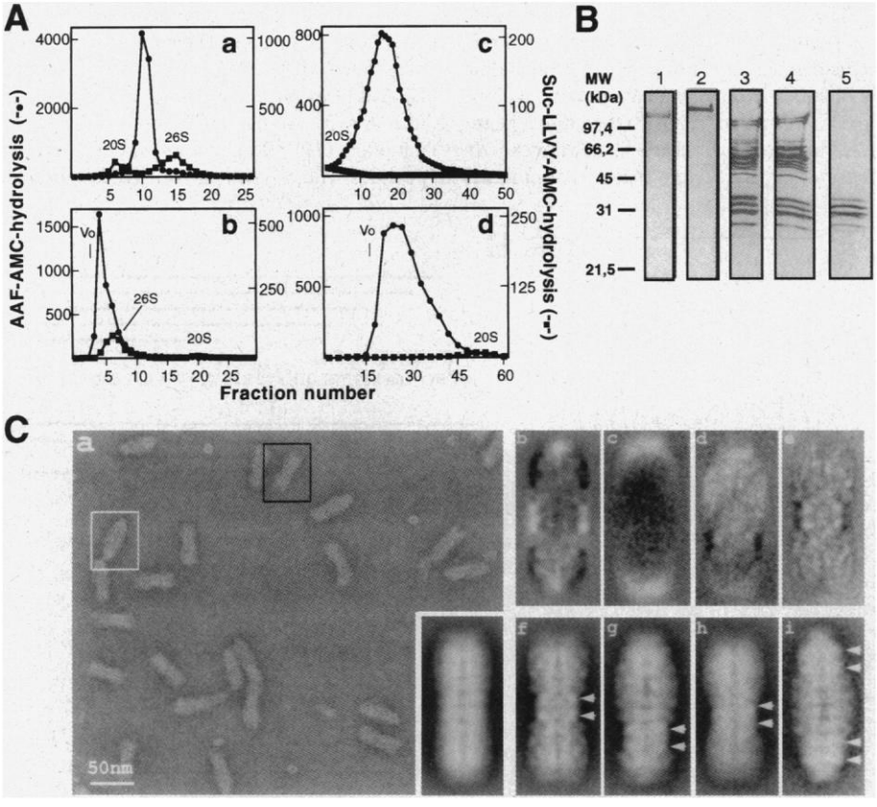

Fig. 1. Isolation and structural characterization of a HMW AAF-AMC–hydrolyzing protease copurifying with 26*S* proteasomes. (**A**) HMW proteins obtained from EL4 cytosol by 5 hours of ultracentrifugation were separated on analytical columns (a and b) or (after 3 hours of ultracentrifugation) on preparative columns (c and d). The maximum of AAF-AMC–hydrolyzing activity is sedimented at 100,000*g* in 1 to 3 hours, and 26*S* proteasomes sediment in 5 hours. (a) A massive peak of AAF-AMC–hydrolyzing peptidase activity elutes on a Mono Q–anion-exchange column between 20*S* and 26*S* proteasomes. Proteasomes were detected by their Suc-LLVY-AMC–hydrolyzing activity. The gradient step between 32 and 47% of eluent B is shown. (b) The HMW AAF-AMC–hydrolyzing activity elutes from Superose 6 size-exclusion columns just before the 26*S* proteasomes. (c) For large-scale purification (*3*), the HMW AAF-AMC–hydrolyzing activity was sedimented completely by 3 hours of ultracentrifugation at 100,000*g*. Resuspended material was separated on a Mono Q–anion exchange column. The gradient step between 37 and 40% of eluent B is shown. (d) Fractions containing AAF-AMC–hydrolyzing activity were further purified on a Superose 6 column. Suc-LLVY-AMC–hydrolyzing activity is shown on an expanded scale in order to visualize fractions containing proteasomes. (**B**) SDS–polyacrylamide gel electrophoresis and silver staining of β-galactosidase (116 kD) (lane 1), purified TPPII (lane 2), fast- and slow-running electrophoretic isoforms of 26*S* proteasomes (lanes 3 and 4, respectively), and purified 20*S* proteasomes (lane 5). (**C**, a) Electron micrograph of a TPPII preparation negatively stained with uranyl acetate. White box, particle with an ovoid shape; black box, dumbbell-shaped particle. (**Inset**) Global average of the data set from 1365 individual particles. (b to e) The dominant variances resulting from an eigenvector-eigenvalue image classification. (f to i) Class averages of the predominant conformers of TPPII. Constrictions are indicated by arrows.

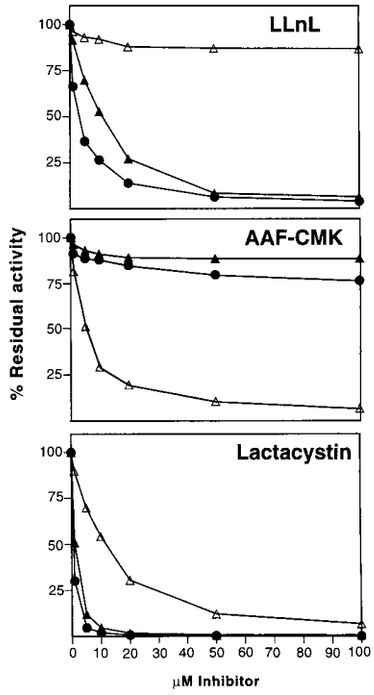

Fig. 2. Inhibition of proteasomes and of TPPII by various protease inhibitors. Purified preparations of mouse 20*S* proteasomes (closed symbols) and of mouse TPPII (open symbols) were incubated with increasing concentrations of the inhibitors LLnL, AAF-CMK, and lactacystin for 45 min at 37°C, followed by determination of the Suc-LLVY-AMC– (●) and AAF-AMC–hydrolyzing activities (▲) of proteasomes and the AAF-AMC–hydrolyzing activity of TPPII (△).

not exclusively, trypsin-like. The cleavage pattern clearly differs from that generated by proteasomes. Major proteasome cleavage sites lie after L_{43}, I_{53}, R_{58}, F_{59}, L_{62}, D_{67} (*14*). Moreover, the trypsin-like activity of proteasomes prefers arginine (R) over lysine (K), whereas TPPII also efficiently cleaves after lysine (K). Similar results were obtained with a second polypeptide substrate. The cleavage patterns observed with biochemically purified and with immunoprecipitated TPPII were similar (compare Fig. 4A and 4C). The degradation of polypeptide substrates was blocked by the serine proteinase inhibitor phenylmethylsulfonyl fluoride and by AAF-CMK (*13*). Combined amino-exopeptidase and endopeptidase activity of proteases is not unprecedented, and cathepsin H, BANA hydrolase, and dipeptidyl peptidase IV have been termed "aminoendopeptidases" (*15*).

It remains to be determined whether TPPII accounts for the HMW AAF-AMC–hydrolyzing protease recognized by Glas *et al.* that appeared to be essential for survival of EL4 cells adapted to LLL(VS) (*2*). As in that study, we find an enhancement of total AAF-AMC–hydrolyzing activity of similar magnitude for whole cells. However, we see considerable AAF-AMC–hydrolyzing activity in HMW fractions of lysates of normal, untreated EL4 cells (Figs. 1 and 3), whereas Glas *et al.* did not. This suggests that factors in addition to TPPII are required for survival of the "adapted" cells. For example, proteasome inhibitors induce apoptotic cell death in proliferating cells (*16*). Thus, the few EL4 cells surviving the initial inhibitor treatment presumably have high antiapoptotic potential. Proteasome inhibitors also strongly induce heat shock protein chaperones (*17*), which clear unfolded polypeptides by refolding or by targeting them to proteases. In addition, proteases other than TPPII may also contribute to survival and proliferation of the resistant cells. TPPII and perhaps other proteases may be highly expressed in the few surviving cells or become induced upon accumulation of misfolded polypeptides during the adaptation process.

The physiological functions of cytosolic TPPII are not known. TPPII may play a role in the degradation of oligopeptides, including cytotoxic T lymphocyte epitopes and epitope precursors, given its high tripeptidyl peptidase activity toward such substrates (*8*). These oligopeptides are mainly the products of proteasome-mediated proteolysis. Although TPPII is not an obvious molecular homolog of the archaebacterial Tricorn protease, it may act as a functional homolog in eukaryotes. The Tricorn protease acts at post-proteasomal steps of protein degradation in archaebacteria (*18*). Because purified TPPII can degrade polypeptides, it may also participate in the degradation of a proportion of cytosolic proteins.

To wat extent can TPPII substitute for loss of proteasome functions? In cells with impaired proteasomal function, TPPII may contribute to the degradation of accumulating misfolded proteins and protein fragments resulting from partial digestion by residual proteasomes. TPPII may also generate epitopes or epitope precursors. The peptide loading of the related MHC class I alleles HLA-A3 and HLA-A11 is not impaired when the trypsin-like activity of the proteasome is severely inhibited (*19*). Both alleles strongly prefer peptides with a lysine in the COOH-terminal

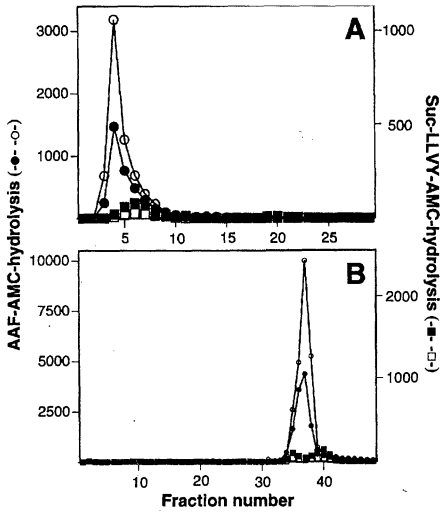

Fig. 3. The AAF-AMC–hydrolyzing activity of TPPII is increased in lactacystin-adapted cells. Cytosolic HMW proteins of lactacystin-adapted (open symbols) and control (solid symbols) EL4 cells were fractionated by Superose 6 gel filtration (**A**) or on a Mono Q–anion exchange (**B**) column. A linear gradient from 0 to 500 mM NaCl of eluent B was used for anion-exchange chromatography. Fractions were assayed for hydrolysis of the proteasome substrate Suc-LLVY-AMC (squares) or the TPPII substrate AAF-AMC (circles). Suc-LLVY-AMC–hydrolyzing activity is shown on an expanded scale in order to visualize fractions containing proteasomes.

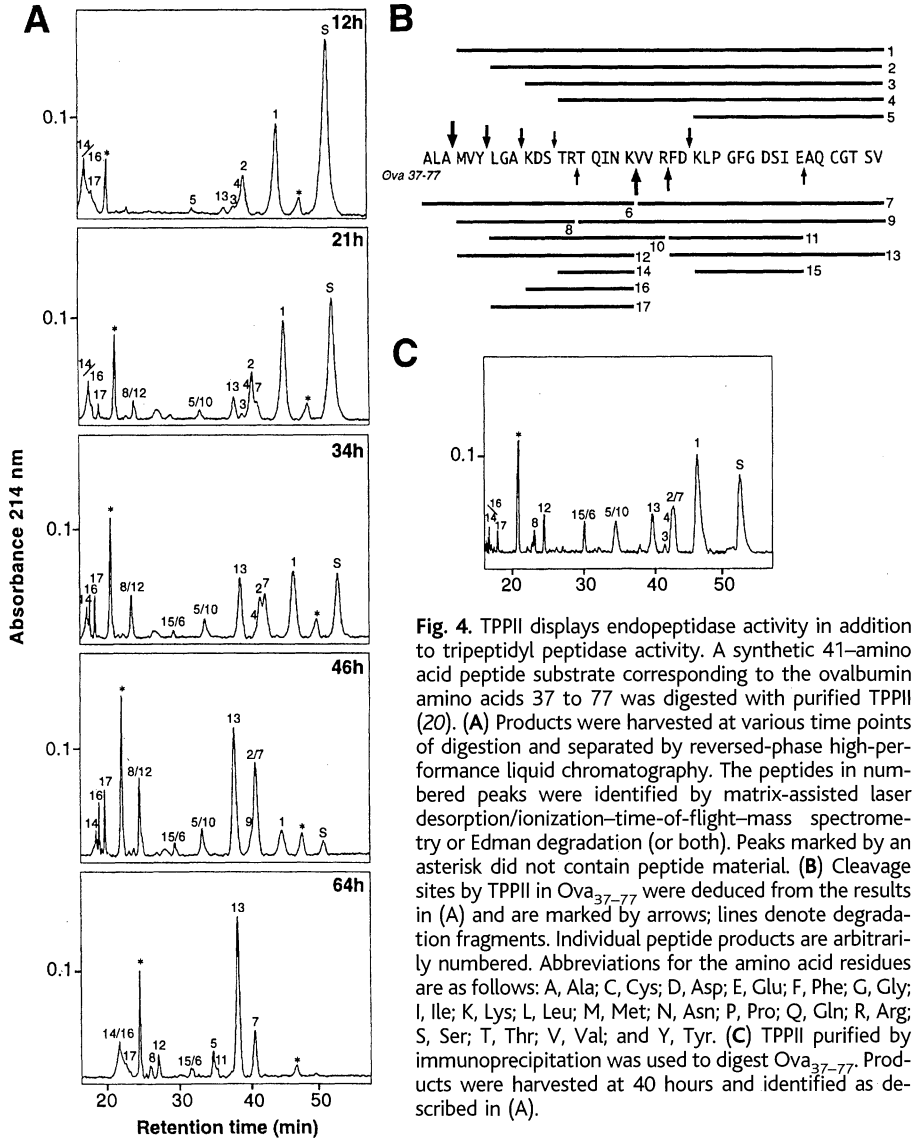

Fig. 4. TPPII displays endopeptidase activity in addition to tripeptidyl peptidase activity. A synthetic 41–amino acid peptide substrate corresponding to the ovalbumin amino acids 37 to 77 was digested with purified TPPII (*20*). (**A**) Products were harvested at various time points of digestion and separated by reversed-phase high-performance liquid chromatography. The peptides in numbered peaks were identified by matrix-assisted laser desorption/ionization–time-of-flight–mass spectrometry or Edman degradation (or both). Peaks marked by an asterisk did not contain peptide material. (**B**) Cleavage sites by TPPII in $Ova_{37–77}$ were deduced from the results in (A) and are marked by arrows; lines denote degradation fragments. Individual peptide products are arbitrarily numbered. Abbreviations for the amino acid residues are as follows: A, Ala; C, Cys; D, Asp; E, Glu; F, Phe; G, Gly; I, Ile; K, Lys; L, Leu; M, Met; N, Asn; P, Pro; Q, Gln; R, Arg; S, Ser; T, Thr; V, Val; and Y, Tyr. (**C**) TPPII purified by immunoprecipitation was used to digest $Ova_{37–77}$. Products were harvested at 40 hours and identified as described in (A).

position, compatible with the endoprotease specificity of TPPII. Most MHC class I–binding peptides have hydrophobic COOH-terminal amino acids generated by proteasomes. However, we have observed occasional endoproteolytic cleavage after hydrophobic amino acids by TPPII as well (*13*). Limited peptide supply may also be compensated by protection of peptides by increased levels of heat shock proteins. In combination, these factors may account for the partially maintained MHC class I expression in LLL(VS)-adapted cells (*2*) and in lactacystin-adapted cells (*13*). Cell-cycle progression and degradation of ubiquitinated proteins appear to continue in the absence of normal proteasome function (*2*). What role TPPII plays in these processes is not yet clear. We envisage multiple compensatory mechanisms operating in cells with compromised proteasomal function.

References and Notes

1. O. Coux, K. Tanaka, A. L. Goldberg, *Annu. Rev. Biochem.* **65**, 801 (1996); A. Ciechanover and A. Schwartz, *Proc. Natl. Acad. Sci. U.S.A.* **95**, 2727 (1998); K. L. Rock *et al.*, *Cell* **78**, 761 (1994); V. J. Palombella, O. J. Rando, A. L. Goldberg, T. Maniatis, *ibid.*, p. 773; R. W. King, R. J. Deshaies, J.-M. Peters, M. W. Kirschner, *Science* **274**, 1652 (1996).
2. R. Glas, M. Bogyo, J. S. McMaster, M. Gaczynska, H. L. Ploegh, *Nature* **392**, 618 (1998).
3. Murine EL4 thymoma cells (8×10^9 to 1×10^{10} cells) were harvested and resuspended at a density of 3×10^7 cells per milliliter in imidazole buffer [20 mM imidazole-HCl (pH 6.8), 100 mM KCl, 20 mM EGTA, 2 mM $MgCl_2$, 10% sucrose, 1 mM adenosine triphosphate (ATP)] and lysed by freeze-thawing. The lysate was differentially centrifuged (15 min at 1500*g*, 15 min at 15,000*g*, 60 min at 100,000*g*, 3 hours at 100,000*g*), and the resulting pellet of HMW proteins was resuspended in 50 mM tris-HCl (pH 7.4), 20% glycerol, 5 mM $MgCl_2$, 0.5 mM β-mercaptoethanol, 1 mM ATP) and stored at −80°C. Samples of the resuspended material were separated on a Mono Q (HR16/10) anion-exchange column [buffer A: 20 mM Hepes (pH 7.2), 15% glycerol, 1 mM ATP; buffer B: 20 mM Hepes (pH 7.2), 15% glycerol, 1 M NaCl, 1 mM ATP] followed by gel filtration on a Superose 6-column [2 cm by 50 cm; elution buffer: 20 mM Hepes (pH 7.2), 100 mM NaCl, 15% glycerol, 1 mM ATP]. All purification steps were carried out at 4°C. Samples of collected fractions were used to measure hydrolysis of Suc-LLVY-AMC and AAF-AMC (*4*).
4. Peptidase assays were performed as described (*14*).
5. The protein was digested with trypsin in a 50 mM NH_4HCO_3, 5 mM $CaCl_2$ buffer containing 33% isotopically labeled $H_2{}^{18}O$. Peptides are isotopically labeled to 33% at their COOH-terminus, thereby allowing COOH-terminal fragments (y-ions) to be distinguished from other fragment ions by their specific $^{16}O/^{18}O$ isotopic distribution. The peptides were sequenced on a API III triple quadrupole instrument (PE-Sciex, Toronto, Canada) equipped with a nanoelectrospray source by differential scanning (M. Wilm, G. Neubauer, L. Taylor, A. Shevchenko, A. Bachi, in preparation).
6. B. Tomkinson, *Biochem. J.* **304**, 517 (1994).
7. C. Rose *et al.*, *Nature* **380**, 403 (1996).
8. R. M. Balöw, U. Ragnasson, Ö. Zetterqvist, *J. Biol. Chem.* **258**, 11622 (1983); R. M. Balöw, B. Tomkinson, U. Ragnarsson, Ö. Zetterqvist, *ibid.* **261**, 2409 (1986); E. Macpherson, B. Tomkinson, R. M. Balöw, S. Höglund, Ö. Zetterqvist, *Biochem. J.* **248**, 259 (1987).
9. J. Walz *et al.*, *J. Struct. Biol.* **121**, 19 (1998).
10. P. C. Ramos *et al.*, *Cell* **92**, 489 (1998).
11. T. Tamura *et al.*, *Science* **274**, 1385 (1996).
12. G. Fenteany *et al.*, *ibid.* **268**, 726 (1995).
13. E. Geier, K. Eichmann, G. Niedermann, data not shown.
14. G. Niedermann *et al.*, *Proc. Natl. Acad. Sci. U.S.A.* **93**, 8572 (1996).
15. H. Kirschke *et al.*, *Acta Biol. Med. Ger.* **36**, 185 (1977); T. Nishimura, A. Okitani, R. Katakai, H. Kato, *Eur. J. Biochem.* **137**, 23 (1983); F. Bermpohl, K. Löster, W. Reutter, O. Baum, *FEBS Lett.* **428**, 152 (1998).
16. S. Imajoh-Ohmi *et al.*, *Biochem. Biophys. Res. Commun.* **217**, 1070 (1995); X. Wang, H. Luo, H. Chen, W. Duguid, J. Wu, *J. Immunol.* **160**, 788 (1998).
17. M. Zhou, X. Wu, H. N. Ginsberg, *J. Biol. Chem.* **271**, 24769 (1996); K. T. Bush, A. L. Goldberg, S. K. Nigam, *ibid.* **272**, 9086 (1997); A. B. Meriin, V. L. Gabai, J. Yaglom, V. I. Shifrin, M. Y. Sherman, *ibid.* **273**, 6373 (1998).
18. N. Tamura, F. Lottspeich, W. Baumeister, T. Tamura, *Cell* **95**, 637 (1998).
19. A. H. Benham, M. Gromme, J. Neefjes, *J. Immunol.* **161**, 63 (1998).
20. For each time point, 6 ng of TPPII was incubated with 3 μg of synthetic peptide corresponding to the ovalbumin amino acids 37 to 77 at 37°C in a total volume of 100 μl of assay buffer [20 mM Hepes (pH 7.8), 1 mM EGTA, 0.5 mM EDTA, 5 mM $MgCl_2$, 0.5 mM 2-mercaptoethanol, 5% glycerol]. The analysis of peptide products was performed as described (*14*).

21. We thank S. Gaedicke for technical assistance, E. J. Corey for supplying lactacystin, K. Peters and A. Würch for helpful discussions, and I. Haidl for critical reading of the manuscript. Supported by a grant of the Deutsche Forschungsgemeinschaft (NI 368/2-1) to G.N.

15 September 1998; accepted 15 January 1999

Role of NADH Shuttle System in Glucose-Induced Activation of Mitochondrial Metabolism and Insulin Secretion

Kazuhiro Eto,[1] Yoshiharu Tsubamoto,[1] Yasuo Terauchi,[1] Takuya Sugiyama,[1] Takuya Kishimoto,[2] Noriko Takahashi,[1] Naoko Yamauchi,[3] Naoto Kubota,[1] Shigeo Murayama,[4] Toru Aizawa,[5] Yasuo Akanuma,[6] Shinichi Aizawa,[7] Haruo Kasai,[2] Yoshio Yazaki,[1] Takashi Kadowaki[1]*

Glucose metabolism in glycolysis and in mitochondria is pivotal to glucose-induced insulin secretion from pancreatic β cells. One or more factors derived from glycolysis other than pyruvate appear to be required for the generation of mitochondrial signals that lead to insulin secretion. The electrons of the glycolysis-derived reduced form of nicotinamide adenine dinucleotide (NADH) are transferred to mitochondria through the NADH shuttle system. By abolishing the NADH shuttle function, glucose-induced increases in NADH autofluorescence, mitochondrial membrane potential, and adenosine triphosphate content were reduced and glucose-induced insulin secretion was abrogated. The NADH shuttle evidently couples glycolysis with activation of mitochondrial energy metabolism to trigger insulin secretion.

Glucose metabolism through glycolysis in the cytosol and then through the tricarboxylic acid (TCA) cycle in mitochondria has been proposed to promote glucose-induced insulin secretion through generation of metabolic signals such as adenosine triphosphate (ATP) or an increase in the ratio of ATP to adenosine diphosphate (ADP) in pancreatic β cells (*1*). However, pyruvate, an end-product of aerobic glycolysis, fails to stimulate insulin secretion, although it can be oxidized in islets as efficiently as glucose (*2*). Studies with an inhibitor of pyruvate transport into mitochondria or an inhibitor of the TCA cycle suggest that metabolism of glucose-derived pyruvate in mitochondria or in the TCA cycle is not well correlated with glucose-induced insulin secretion (*3*). These findings imply that one or more factors derived from glycolysis other than pyruvate are required for the generation of mitochondrial signals that lead to insulin secretion. One candidate for these metabolic coupling factors is NADH generated by the glycolytic enzyme glyceraldehyde 3-phosphate dehydrogenase (GAPDH) (*4*). The cytosolic NADH is transferred into mitochondria for oxidative metabolism and ATP production through two NADH shuttles, the

[1]Department of Internal Medicine; [2]Department of Physiology; [3]Department of Pathology; [4]Department of Neurology, Graduate School of Medicine, University of Tokyo, 7-3-1 Hongo, Bunkyo-ku, Tokyo 113, Japan. [5]Department of Geriatrics, Endocrinology and Metabolism, Shinshu University School of Medicine, 3-1-1 Asahi, Matsumoto 390, Japan. [6]Institute for Diabetes Care and Research, Asahi Life Foundation, 1-6-1 Marunouchi, Chiyoda-ku, Tokyo 100, Japan. [7]Department of Morphogenesis, Institute of Molecular Embryology and Genetics, Kumamoto University School of Medicine, 4-24-1 Kuhonji, Kumamoto 862, Japan.

*To whom correspondence should be addressed. E-mail: kadowaki-3im@h.u-tokyo.ac.jp